Accelerated Publications

X-ray Absorption Spectroscopy on Layered Photosystem II Membrane Particles Suggests Manganese-Centered Oxidation of the Oxygen-Evolving Complex for the S_0-S_1, S_1-S_2, and S_2-S_3 Transitions of the Water Oxidation Cycle†

Lucia Iuzzolino,‡,§ Jens Dittmer,‡ Wolfgang Dörner,‡,§ Wolfram Meyer-Klaucke,|| and Holger Dau*,‡

FB Biologie/Botanik, Philipps-Universität Marburg, Lahnberge, D-35032 Marburg, Germany, FB Chemie, Philipps-Universität Marburg, Lahnberge, D-35032 Marburg, Germany, and European Molecular Biology Laboratory, Hamburg Outstation, Notkestrasse 85, D-22603 Hamburg, Germany

Received July 20, 1998; Revised Manuscript Received September 14, 1998

ABSTRACT: By application of microsecond light flashes the oxygen-evolving complex (OEC) was driven through its functional cycle, the S-state cycle. The S-state population distribution obtained by the application of *n* flashes ($n = 0 \ldots 6$) was determined by analysis of EPR spectra; Mn K-edge X-ray absorption spectra were collected. Taking into consideration the likely statistical error in the data and the variability stemming from the use of three different approaches for the determination of edge positions, we obtained an upshift of the edge position by 0.8−1.5, 0.5−0.9, and 0.6−1.3 eV for the S_0-S_1, S_1-S_2, and S_2-S_3 transitions, respectively, and a downshift by 2.3−3.1 eV for the S_3-S_0 transition. These results are highly suggestive of Mn oxidation state changes for all four S-state transitions. In the S_0-state spectrum, a clearly resolved shoulder in the X-ray spectrum around 6555 eV points toward the presence of Mn(II). We propose that photosynthetic oxygen evolution involves cycling of the photosystem II manganese complex through four distinct oxidation states of this tetranuclear complex: Mn(II)−Mn(III)−$Mn(IV)_2$ in the S_0-state, $Mn(III)_2-Mn(IV)_2$ in the S_1-state, $Mn(III)_1-Mn(IV)_3$ in the S_2-state, and $Mn(IV)_4$ in the S_3-state.

The earth's dioxygen atmosphere has been produced by photosynthetic water oxidation at a tetranuclear manganese complex, which is bound to the polypeptides of photosystem II (PS II). This manganese complex together with the part of the PS II protein complex directly involved in photosynthetic water splitting is denoted as "oxygen-evolving complex" (OEC);[1] structure and location of the OEC and the functional role of the four manganese ions are currently the subjects of intensive research (*1*−*6*).

Successively absorbed photons drive the cycling of the OEC through four semistable states: S_1 (dark state) → S_2 → S_3 → S_0 → S_1 → ... (*7*). The S_3-S_0 transition is assumed to involve the formation of a transient intermediate state, the S_4; the S_4-S_0 transition is coupled to the release of dioxygen. The question of how manganese oxidation state changes are involved in the light-driven cycling of the OEC is of crucial importance with respect to the mechanism of photosynthetic water oxidation.

Data obtained by various techniques indicate that the S_0-S_1 and the S_1-S_2 transitions involve manganese oxidation, whereas the $S_3-S_4-S_0$ transition is coupled to an overall reduction of manganese ions. However, it is still a highly controversial issue whether the S_2-S_3 transition involves manganese oxidation (see refs *5*, *8*, and *9* and the Discussion).

Measurement and analysis of X-ray edge spectra can facilitate the characterization of the oxidation state of protein-bound metals because, in general, the edge position is shifted to higher energies upon oxidation of the X-ray absorbing metal ion. A preferential population of the S_2-, S_3-, or S_0-state is achievable by the application of one, two, or three light flashes, respectively. Combining the X-ray edge and the light flash approach, Ono et al. (*10*) obtained results which appear to prove manganese oxidation upon the S_2-S_3 transition. However, as correctly pointed out by Roelofs et al. (*11*), the investigation of Ono et al. (*10*) is not beyond criticism because no independent information on the actual S-state distribution had been available. Roelofs et al. (*11*)

† This research was supported by the German Bundesministerium für Bildung und Forschung (program: Erforschung kondensierter Materie, Verbund 48) and the Deutsche Forschungs-Gemeinschaft (Marburger Graduiertenkolleg "Enzymchemie"). W.D. received financial support in the form of a fellowship of the Studienstiftung des deutschen Volkes.

* To whom correspondence should be addressed. Phone: +49-6421-282078. Fax: +49-6421-282057. E-mail: dauh@mailer.uni-marburg.de.

‡ FB Biologie/Botanik, Philipps-Universität Marburg.

§ FB Chemie, Philipps-Universität Marburg.

|| Hamburg Outstation.

[1] Abbreviations: Chl, chlorophyll; Cyt_{b559}, cytrochrome which is an integral part of the PS II; DMSO, dimethyl sulfoxide; EPR, electron paramagnetic resonance; EXAFS, extended X-ray absorption fine structure; MES, 2-(*N*-morpholino) ethanesulfonic acid; OEC, oxygen-evolving complex; PPBQ, phenyl-*p*-benzoquinone; PS, photosystem; Tyr_D, Tyr_Z specific tyrosine residues of the PS II; XAS, X-ray absorption spectroscopy.

10.1021/bi9817360 CCC: $15.00
Published on Web 11/14/1998

used the magnitude of the S_2-state multiline signal (*12*), an EPR signal which is under the chosen experimental conditions present only in the S_2-state of the OEC, for the determination of the actual S-state composition. In clear contrast to Ono et al. (*10*), they concluded that probably no direct manganese oxidation is involved in the S_2-S_3 transition. The X-ray results of Roelofs et al. (*11*) appeared to settle the disputed question. In this study, however, we demonstrate that there is, indeed, a pronounced shift of the X-ray edge position, strongly suggesting manganese oxidation upon the S_2-S_3 transition.

Whereas in refs *10* and *11* suspensions of PS II membrane particles are used, we investigate the manganese oxidation state changes using multilayers of PS II membrane particles (see, e.g., ref *13*). We consider the X-ray properties of these samples and the illumination conditions of this investigation to be more favorable with respect to the correct assessment of the S-state composition by EPR spectroscopy. Furthermore, the possible influence of statistical errors related to the collection of X-ray spectra and to the accuracy of the determination of the S-state composition by EPR spectroscopy is assessed; several alternative approaches for the determination of X-ray edge positions are applied.

MATERIALS AND METHODS

Preparation of "Flashed" Samples. With the exception of the following modifications, layered PS II membrane particles were prepared as described elsewhere (*13*). The spinach thylakoid membranes were incubated for 1 min in the Triton X-100 buffer (detergent-to-chlorophyll ratio of 25 mg/mg of Chl; 1 M glycine betaine, 15 mM NaCl, 10 mM $MgCl_2$, 5 mM $CaCl_2$, 25 mM MES, pH 6.2) and washed 3−4 times by centrifugation and resuspension in the detergent-free buffer B (1 M glycine betaine, 15 mM NaCl, 5 mM $MgCl_2$, 5 mM $CaCl_2$, 25 mM MES, pH 6.2). For the final pellet we determined an oxygen evolution activity of 1200−1400 μmol of O_2/((mg of Chl) h) at 28 °C. Frequently, thick suspensions of PS II membrane particles (3−4 mg of Chl/mL) were stored at −70 °C; frozen suspensions were slowly thawed and washed by resuspension (in buffer B) and centrifugation. The pellet was resuspended in buffer B plus 10% (v/v) glycerol and 150 nmol of PPBQ/mg of Chl, using a stock solution of 30 mM PPBQ in DMSO, and layered membrane particles were prepared using a special centrifugation procedure (*13*). Immediately after the centrifugation a single light flash (preflash) was applied (as described below), the samples were placed in a desiccator for 2 h (without desiccant and in complete darkness), and the drying process was accelerated by mildly evacuating once (at the beginning of the 2 h drying period). Noteworthy is that the centrifuge-and-dry procedure used here results in only partially dried samples without any texture, whereas for paint-and-dry procedures the brush texture is likely to be related to significant (and irreproducible) spacial variations in the sample thickness.

Two microsecond flash lamps (FX 134 of EG&G Electro Optics; electrical pulse energy of 4.5 J/lamp; full-width at half-maximum of 5 μs) were employed for simultaneous flash illumination of the sample from two sides: the backside consisting of a Kapton tape (which forms the backwall of the sample holder) and the open frontside. Because the light flash from the backside had to pass through the Kapton tape and because Kapton acts as an efficient long pass filter with a 50% cutoff wavelength of 500 nm, the front face was also illuminated through a Kapton foil.

Two hours before application of a flash sequence, all samples were exposed to a single "preflash" and subsequently placed in complete darkness (in the desiccator described above at 5 °C). After illumination at 5 °C with a sequence of n flashes ($n = 0-6$, flash frequency of 1 Hz), the illuminated sample was shot into liquid nitrogen within clearly less than 1 s (using a device built by the mechanics workshop of the FB Biologie, Marburg). The ensemble of samples prepared on a single day is in the following referred to as a "flash series".

EPR Measurements. Conditions and instrumentation for the collection of X-band EPR spectra are described elsewhere (*14*). The so-called multiline signal was measured at 8.5 K (μ-wave power of 32 mW and 12.5 kHz field modulation with a modulation amplitude of 20 G). For the glycerol-containing samples we never observed any indications for a S_0-state multiline signal (*15*, *16*). For precise quantification of the magnitude of the S_2-state multiline signal a correlation method has been applied which is described elsewhere (*17*). The results obtained by this correlation method are, in principle, equivalent to the results obtainable by signal quantification through averaging of the peak-to-trough amplitudes of the multiline EPR signal (as carried out in ref *11*). However, the correlation method (*17*, *18*) is superior with respect to the suppression of undesired noise contributions. By using this method, we detect a few percent of PS II's in the S_2-state prior to application of the flash sequence which might have escaped an analysis based on the peak-to-trough method. This residual S_2-state population, $[S_2]^0$, is considered in the simulations of the flash number dependence of the S-state multiline signal amplitude which are described in the context of Figure 1.

X-ray Absorption Spectroscopy. The X-ray measurements were carried out at the EMBL beam line D2 (HASYLAB, DESY, Hamburg, Germany) largely as described elsewhere (*13*). X-ray fluorescence excitation spectra were collected at two distinct excitation angles (either 15° or 55°; angle between the X-ray electric field vector and the normal to the surface of PS II particles multilayers) using an energy-resolving 13-element solid-state detector. The total count rate per element channel was 1000−5000 counts/s. For excitation energies above the Mn K edge, the mean Mn fluorescence count rates per element channel were, typically, 250 and 175 counts/s for excitation at 15° and 55°, respectively. For excitation below the Mn K edge, the mean count rates were around 45 and 30 counts/s at 15° and 55°, respectively. In the following the measured fluorescence excitation spectra are referred to as X-ray absorption spectra.

The X-rays passing the cryostat were used to measure the absorption spectrum of a $KMnO_4$ powder enclosed in Kapton tape and placed in front of an ion chamber. The $KMnO_4$ powder exhibits a sharp pre-edge peak which is assumed to be at 6543.30 eV. By using a least-squares fit using a Gaussian function and a second-order background polynomial, we determined the position of the $KMnO_4$ pre-edge peak on a preliminary energy-scale with an estimated precision of 0.02 eV; the energy scale of the collected X-ray

spectra was corrected accordingly.

During the X-ray measurements, the temperature inside the He cryostat had been 17−20 K; heat exchange was facilitated by He gas. We observed a shift of the Mn K edge by about 0.1 eV/h in zero-flash samples and about 0.2 eV/h in samples exposed to one or more flashes. The heat-exchange gas pressure, which had been either 60 or 600 mbar, did not affect the rate of manganese X-ray photoreduction significantly.

The rapid X-ray photoreduction and its oxidation state dependence are extremely problematic in the context of the present investigation. To minimize the influence of photoreduction, we typically did not use more than two energy scans (about 20 min of X-ray illumination per scan) per sample position for the subsequent data analysis. For each flash state, S^n, ($n = 0$ ... 5, number of applied microsecond flashes) of an individual series, usually 2−4 scans were measured on different samples and utilized for the analysis of edge positions.

In this investigation, the mean energy, E^{mean}, of the increase in the normalized absorption, $\mu(E)$, from μ_1 to μ_2 is used to determine the position of the X-ray edge:

$$E^{mean} = \frac{1}{\mu_2 - \mu_1} \int_{\mu_1}^{\mu_2} E(\mu)\, d\mu \qquad (1)$$

where $E(\mu)$ is the inverse function of the normalized absorption, $\mu(E)$. The computational approach to circumvent the problems associated with the use of the inverse function is described elsewhere (*19*). We have chosen the following: $\mu_1 = 0.15$ and $\mu_2 = 1.0$; this choice of the integration limits enables the application of eq 1 to manganese redox enzymes and various inorganic manganese compounds (*19*).

Using the edge spectra of pure S-states (equally spaced data points, point spacing of 0.14 eV) for the calculation of the second derivatives shown in Figure 3B the following procedure was employed: (1) smoothing by calculation of the running average over 13 points (corresponding to 1.8 eV), (2) calculation of the first-derivative spectrum, (3) running average (13 points), (4) running average (13 points), (5) calculation of derivative yields the second-derivative spectrum, (6) running average (13 points), and (7) running average (13 points). The edge positions obtained by the "second-derivative method" (Table 3) are the energies of the zero crossing points of the second-derivative spectra.

RESULTS

Determination of S-State Composition. In this investigation, S-state cycling is achieved by the application of sequences of microsecond light flashes. Ideally, in dark-adapted samples all PS II's are in the S_1-state; each flash results in the advancement of all PS II's to the subsequent state of the cycle. Such a fully synchronized cycling of all PS II's, however, cannot be achieved. Thus, special efforts are required for optimizing the S-state compositions and correct determination of the achieved S-state composition.

In dark-adapted PS II's the S_1-state prevails. Usually, however, there is a residual S_0-state population (<25%). Exploiting that higher S-states relax toward S_1 whereas the S_1-state is dark-stable, the S_1-state population was maximized by application of a single preflash and subsequent relaxation (for 2 h at 5 °C).

If the first light flash of a flash sequence drove the formation of the Tyr_D radical, the determination of the resulting S-state composition would be more intricate. To ensure formation of the Tyr_D radical in all PS II's prior to application of the flash sequence, Roelofs et al. (*11*) applied two preflashes. We found in our preparations the Tyr_D radical to be present in most PS II's already before application of the preflash. Therefore, a single preflash is sufficient to obtain a PS II state composition characterized by oxidized Tyr_D in essentially all PS II's (no further increase in the Tyr_D radical EPR signal is detectable) and a maximal population of the S_1-state.

For determination of the S-state composition we employed the approach of Roelofs et al. (*11*) which is briefly outlined in the following. Photosystems in the S_2-state give rise to a characteristic EPR signal around $g = 2$, the so-called multiline signal (*12*). The $g = 4$ signal, which is also associated with the S_2-state, is not observed because formation of this signal is inhibited due to the presence of glycerol. Therefore, the magnitude of the S_2-state multiline signal is proportional to $[S_2]$, the fraction of PS II's in the S_2-state. Application of a flash sequence causes S-state cycling and thus an oscillatory pattern in $[S_2]$ which is reflected by the oscillations in the magnitude of the multiline EPR signal (see Figure 1A). The oscillatory pattern is simulated using a relatively simple model involving a miss parameter, *M* (probability that PS II's fail to advance in the S-state cycle), and a double-hit parameter, *D* (probability for advancement by two S-states). The achieved agreement between the simulated and the experimentally obtained oscillation pattern suggests that the model is sufficiently accurate (see Figure 1A); the use of more complex models (e.g., ref *20*) seems not to be required. By a least-squares curve-fit approach the parameters for optimal agreement between simulation and experiment are determined. Eventually these parameters allow calculation of the S-state composition obtained by illumination with *n* flashes ($n = 0, 1, ...$).

Analysis of Edge Position Flash Pattern. After determination of the S-state composition, X-ray absorption spectra were collected; the position of the Mn K edge was determined by the integral method described in Materials and Methods. The flash number dependence of the measured edge positions is presented in Figure 1B (for both excitation angles); the full X-ray edge spectra obtained by application of 0, 1, 2, and 3 flashes are shown in Figure 2 (for excitation at 55°). The difference in the absolute values of the edge positions for excitation at 55° and 15° reflects the known dichroism (meaning excitation angle dependence) of the absorption edge shape of the PS II manganese complex (*21*, *22*).

The excitation angle of 55° corresponds to the so-called magic angle (54.7°; refs *23* and *24*). Magic angle spectra of "oriented" PS II samples (preferential orientation of the molecular system with respect to a macroscopic axis) are predicted and found (data not shown) to resemble closely the corresponding spectra of "isotropic" suspensions. The dichroism in the absorption edge of the PS II manganese complex is, essentially, not understood (*21*). Here, the results obtained for an excitation angle of 15° are presented because they supplement and confirm the magic angle results.

On the basis of the S-state compositions determined by analysis of the multiline pattern as described above, absolute

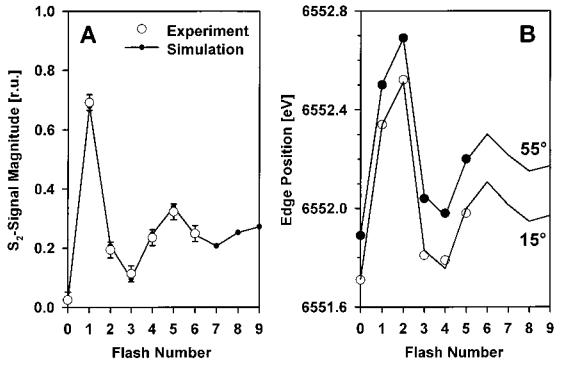

FIGURE 1: Magnitude of the S_2-state multiline EPR signal (A) and edge positions (B) versus the number of microsecond flashes. (A) For each flash number several samples of a single flash series have been analyzed. The resulting mean values are presented as open circles; the vertical bar represents the averaged standard deviation. By a least-squares fit of the simulated pattern to the data point (see Materials and Methods), the solid line has been obtained. For the EPR data set shown, the fit results in 14% and 15% for the miss parameter, *M*, and the double-hit parameter, *D*, respectively. (B) Edge positions versus number of microsecond flashes for two X-ray excitation angles: 55° (closed circles) and 15° (open circles). The mean values of the edge positions of 6 flash series (per excitation angle) are shown. With the use of the (averaged) S-state compositions, the solid lines have been obtained by variation of the S-state edge energies and minimization of the error sum (least-squares fit). The fit procedure delivers the edge energies, E_i, for the "pure" S-states (15° values in parentheses): $E_0 = 6550.77$ (6550.43), $E_1 = 6551.92$ (6551.75), $E_2 = 6552.55$ (6552.39), and $E_3 = 6553.53$ (6553.40).

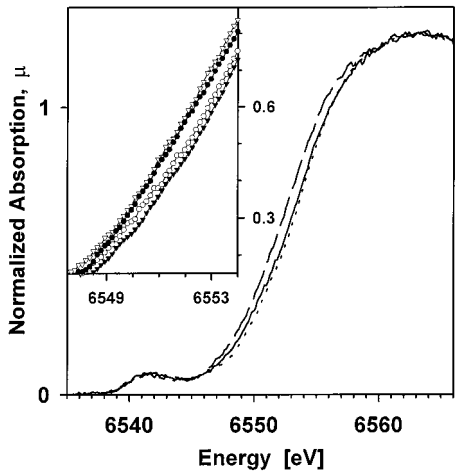

FIGURE 2: Edge spectra as obtained by application of 0, 1, 2, and 3 microsecond flashes: zero-flash sample, broken line and filled circles; single flash, solid line and open circles; two flashes, dotted line and closed triangles; three flashes, open triangles (for clarity shown in the inset only). In the two-flash sample the S_3-state is preferentially populated, but due to double hits (see Table 1), a significant S_0-state population is already present. Therefore, the edge shift caused by the second flash is smaller than the edge shift caused by the first flash. The pure S-state spectra obtained by deconvolution of the spectra shown here are presented in Figure 3.

edge positions were determined for "pure" S-states by simulation of the observed edge shift (Figure 1B). For magic angle excitation, the best agreement between simulated data and experimental results for the averaged edge positions indicates a shift of the absorption edge by 1.15 eV for the S_0-S_1 transition, by 0.63 eV for the S_1-S_2 transition, and by 0.98 eV for the S_2-S_3 transition. For excitation at 15°, edge shifts of 1.32, 0.64, and 1.01 eV are found.

The measured EPR and X-ray spectra are not noise-free. Therefore, the precision of the quantification of the EPR signal amplitude and of the edge position is limited. Both inprecisions may cause a statistical error in the eventually determined edge positions of the pure S-states. To determine the precision in the edge positions of the pure S-states (meaning the likely magnitude of the statistical error due to noise in the data), each individual flash series has been evaluated separately; the results are summarized in Table 1. The mean values indicate clear edge shifts for all S-state transitions; for all transitions the "likely error" (or the "uncertainty range") is small in comparison to the observed shift.

(It should be noted that the limited precision of the analysis of the multiline pattern is not the sole source of the "scatter" in *M* and *D*. We observed differences in the oscillation characteristics of different flash series which are presumably due to small variations (±10%) in the amount of Chl used in the last centrifugation step and, consequently, in the optical thickness of the samples. Furthermore, in some flash series the intensity of the flash illumination was increased due to a reduced distance between flash lamp and sample surface. Because the origin of the *M* and *D* scatter is not purely stochastic noise, no "likely error" for *M* and *D* is presented in Table 1.)

We found no indication that the double-hit parameter, *D*, and the miss parameter, *M*, determined by analysis of the multiline flash dependence are inaccurate. Nonetheless, in the following we consider the possibility that the correct values of *D* and *M* differ significantly from the values determined by simulation of the flash number dependence of the EPR signal amplitude. The parameters *M* and *D* were varied by the standard deviations of Table 1, and the S-state edge energies were determined by a fit of the experimental edge energy pattern; the resulting edge shifts and the corresponding error sum are shown in Table 2. We conclude that, even if there were a significant error in the determined values of *M* and *D*, the central result of this investigation (i.e., occurrence of a significant edge shift upon the S_2-S_3 transition) would be, qualitatively, the same.

Another conclusion can be drawn on basis of Table 2. Variations of *M* and *D* result in increased deviations between the simulated and the experimentally determined X-ray edge pattern (pronounced increase in the error sum, fourth column of Table 2). Seemingly the values for *M* and *D* determined by EPR spectroscopy (which are M_0 and D_0) are in the best agreement with the observed oscillations in the edge position. This observation confirms the accuracy of the *M* and *D* determinations by EPR spectroscopy.

Analysis of Deconvoluted Edge Spectra. The averaged spectra obtained for 0, 1, 2, and 3 flashes (Figure 2) and the averaged S-state compositions (determination as described in the context of Figure 1A) have been used for the calculation of pure S-state spectra. The used deconvolution method corresponds to the approach described in ref *11*. The edge spectra obtained for the pure S-states are shown in Figure 3; obviously all S-state transitions are accompanied by a significant shift of the edge position.

There is no single, commonly accepted standard for the determination of edge positions; the energy value obtained for the position of an X-ray edge, the edge energy, depends on the approach used. In the following, the results obtained

Table 1: X-ray Edge Shifts Determined for Individual Flash Series[a]

	M^b	D^c	$E_1{}^d$	$E_1 - E_0{}^e$	$E_2 - E_1{}^e$	$E_3 - E_2{}^e$	$E_0 - E_3{}^e$
55° − mean[f]	0.22	0.11	6551.93	1.10	0.60	0.92	−2.62
55° − σ[g]	0.029	0.033	0.13	0.38	0.23	0.55	0.61
55° − error[h]			0.05	0.16	0.09	0.22	0.25
15° − mean[f]	0.22	0.11	6551.65	1.02	0.79	0.83	−2.64
15° − σ[g]	0.029	0.033	0.23	0.59	0.36	0.59	0.91
15° − error[h]			0.09	0.25	0.15	0.24	0.37

[a] Six series per excitation angle have been evaluated. [b] Miss parameters obtained by simulation of the S_2-state signal pattern. [c] Double-hit paramaters as obtained by the simulation of the S_2-state signal pattern. [d] Edge position for the S_1-state in eV. [e] Edge shifts in eV. [f] Mean value of six series. [g] Standard deviation. [h] Likely error $= \sigma\sqrt{N}$ with $N = 6$.

Table 2: Sensitivity of Edge Positions toward Variations in *M* and *D* (for 55° Excitation)

	M^a	D^b	$10^3 r^{2c}$	$E_1{}^d$	$E_1 - E_0{}^e$	$E_2 - E_1{}^e$	$E_3 - E_2{}^e$	$E_0 - E_3{}^e$
M_0, D_0[f]	0.215	0.107	0.4	6551.93	1.15	0.63	0.95	−2.73
$M+$, $D+$[g]	0.244	0.140	2.2	6551.97	1.72	0.45	1.65	−3.81
$M+$, $D-$[g]	0.244	0.073	9.8	6551.92	1.01	0.79	0.49	−2.28
$M-$, $D+$[g]	0.187	0.140	4.9	6551.93	1.21	0.45	1.39	−3.05
$M-$, $D-$[g]	0.187	0.073	0.9	6551.90	0.73	0.71	0.56	−1.99

[a] Miss parameter. [b] Double-hit parameter. [c] Sum of squared deviations, r^2, between simulated and experimentally determined edge energies. [d] Edge position for the S_1-state in eV. [e] Edge-shifts in eV. [f] Mean values of *M* and *D* of Table 1. Whereas in Figure 2 averaged S-state populations have been used for the simulation of the edge position pattern, in Table 2 the averaged values of *M* and *D* have been used for the calculation of the S-state compositions. The two approaches result in almost the same S-state compositions and edge energies for the pure S-states. [g] M_0 and D_0 plus or minus the respective standard deviation of Table 1.

by the application of four distinctly different approaches for the determination of edge energies are compared (Table 3).

(1) Edge energies are determined by the integral method described in Materials and Methods. This method is relatively insensitive to changes in the shape of the X-ray spectrum and to noise contributions. Noteworthy is the fact that the edge shifts determined for the deconvoluted spectra are in good agreement with the results (see Figure 1B and Table 1) obtained by simulation of the flash pattern of nondeconvoluted spectra.

(2) The edge position is determined as the zero crossing energy of the second derivative (inflection point energy, see Figure 3B). Often the second-derivative approach is applied because it is relatively insensitive to the background in the spectra which stems from scattered X-rays; the obtained results are independent of the accuracy of the normalization procedure. (Noteworthy is the fact that, for the data presented here, the scattering background has been minimal due to the use of partially dehydrated samples and a special cryostat design. Consequently, background removal and normalization are not critical.) The inflection point energy is sensitive not only to changes in the mean edge energy but also to variations in the shape of the absorption edge (see Discussion). Furthermore, the edge positions determined by the second-derivative method depend highly on the details of the "smoothing procedure" which is required for the calculation of the second derivatives. By application of approximately the same extent of smoothing as used in ref *11* (see Figure 3B), we obtained a particularly pronounced edge shift for the S_0-S_1 transition. In comparison to the first method, the second-derivative approach results in an increased edge shift for the S_1-S_2 transition and a decreased shift for the S_2-S_3 transition. Nonetheless, in contrast to the finding reported in ref *11*, the S_2-S_3 shift is not significantly smaller than the S_1-S_2 shift.

(3) Frequently, the energy corresponding to the half-height of the normalized spectrum is presented (normalization in the EXAFS range to unity). By using this method, we observed the same edge shift magnitude for the S_2-S_3 transition as for the S_1-S_2 transition.

(4) Ono et al. (*10*) defined the edge position as the energy which corresponds to half of the maximal absorption (which is reached around 6560 eV). By using this approach, we obtained results which are in resonably good agreement with the results of Ono et al. (*10*) who determined edge shifts of 1.0, 0.8, and 1.2 eV for the S_0-S_1, S_1-S_2, and S_2-S_3 transitions, respectively.

DISCUSSION

We have determined edge positions of the pure S-states by simulation of the oscillation pattern of the measured edge positions (Figure 1B, Table 1; similar to the approach used in ref *10*) and by analysis of deconvoluted spectra (Table 3; deconvolution approach used in ref *11*). We have examined the uncertainty in the edge shift values which stems from noise in the measured spectra (likely error in Table 1), the influence of hypothetical inaccuracies related to the determination of the S-state composition (Table 2), and the influence of the method used for the determination of edge energies (Table 3). Furthermore, we quantified the influence of X-ray photoreduction and used an experimental protocol which essentially excludes the influence of X-ray photoreduction on the presented results (see Materials and Methods). On these grounds we conclude that the X-ray edge shift for the S_2-S_3 transition of the PS II manganese complex is not significantly smaller than the edge shift for the S_1-S_2 transition. This conclusion is in agreement with ref *10*, but it is in conflict with the more recent findings of ref *11*. Some aspects of the discrepancy are discussed in the following paragraphs.

Influence of the Physical Sample Properties. Roelofs et al. (*11*) used suspensions filled into sample holders of 800 μm depth. Due to absorption and scattering of the exciting

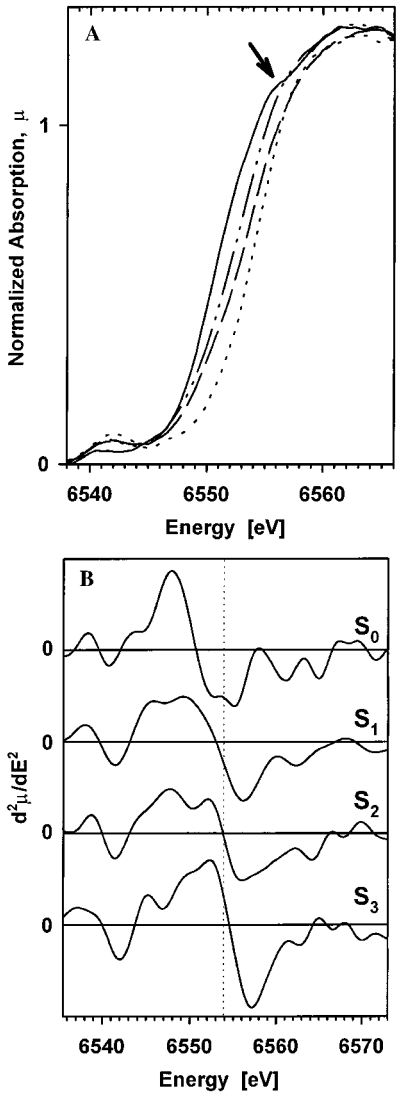

FIGURE 3: Edge spectra of the pure S-states. (A) S_0 (solid line), S_1(broken line with intermediate dots), S_2 (broken line), S_3 (dotted line). The spectra used for the deconvolution have been collected at the magic angle (∼55°). All spectra have been normalized in the EXAFS range. The arrow marks a shoulder which might indicate the presence of Mn(II) in the S_0-state. (B) Second derivatives of the edge spectra of the pure S-states (The used smoothing procedure is described in Materials and Methods; the dotted line indicates the inflection point energy for the S_2-state.)

X-rays (and the X-ray fluorescence by water), most of the fluorescence signal originates from photosystems located within 100−200 μm from the beam-exposed sample surface. Due to the high optical density of the samples, upon illumination with a flash lamp the photosystems located in the front layer (100−200 μm) are exposed to considerably higher photon fluxes than deeper-lying photosystems. This means that in the front layer the light intensity in the tail of the flash lamp light pulse (e.g., at 100 μs after the flash peak) is still sufficient to induce a second turnover in a significant fraction of the photosystems (double hits). In contrast, for deeper-lying photosystems the peak intensity may be subsaturating and a significant fraction of PS II does not experience a single turnover (misses). Consequently, correct characterization of these "front PS II"'s would require a double-hit parameter, *D*, and a miss parameter, *M*, which are increased and decreased, respectively, with respect to the mean values of these parameters as they are determined by EPR spectroscopy. In conclusion, possibly Roelofs et al. (*11*) underestimated *D* and overestimated *M* for the PS II's which give rise to the detected X-ray fluorescence. Smaller values of *D* or larger values of *M*, however, tend to increase the (apparent) S_1-S_2 shift and to decrease the S_2-S_3 shift (see Table 2). In the present investigation the thickness of the partially hydrated samples had been clearly below 100 μm, and the samples had been illuminated from both sides simultaneously. Therefore, there is no significant difference between the mean S-state composition (as determined by EPR spectroscopy) and the S-state composition of the PS II's which give rise to the X-ray fluorescence signal. Because Ono et al. (*10*) used the X-ray data itself for the determination of the miss parameter, their results are, presumably, not significantly affected by the depth dependence of the S-state population distribution.

In the present investigation the mean value of the double-hit parameter *D* had been determined to be 11% (Table 1) whereas Roelofs et al. (*11*) determined a double-hit parameter of 5%. As discussed above, double hits occur mainly in the front layer of the sample which is exposed to particularly high flash light intensities. In the present investigation, *D* is approximately two times larger because the samples had been illuminated from two sides. The *M* parameter of this investigation had been relatively high because the amount of PS II needed for the X-ray absorption experiment requires the use of optically particularly thick samples. In conclusion, the relatively high values of *M* and *D* are explainable by the physical properties of the X-ray samples; there are no indications that these parameters reflect a modified S-state cycle of the PS II (e.g., due to inhibition of S-state transitions).

S_1-State Edge Energy. We determined the inflection point energy for the S_1-state to be 6553.0 eV which is higher by 1.3 eV than the value presented in ref *11*. In ref *11* small amounts of adventitious Mn^{2+} might have shifted the inflection point of the S_1-state spectrum to significantly lower energies (as discussed below). Alternatively, with the use of two preflashes (in ref *11*), double hits could have caused some population of the S_0-state in the zero-flash samples resulting in a downshift of the inflection point energy.

Method for E_i Determination. The X-ray edge spectrum of a manganese compound typically is characterized by a complicated shape which depends on its structure and oxidation state. The edge spectra of the PS II manganese complex are relatively featureless. Nonetheless, all S-state transitions cause not only an edge shift but also a discernible change in the edge shape. Changes in edge shape affect the edge energy values (and edge shifts) obtained by different methods in dissimilar ways (Table 3). Whereas the integral method (*19*), which provides a mean edge energy, is relatively insensitive to mere changes in the edge shape, the results obtained by the second-derivative method are particularly strongly affected by edge shape changes. It is a related disadvantage of the second-derivative method that, for a mixture of manganese compounds (or, e.g., states of the PS II manganese complex), the obtained inflection point energy depends in an intuitively unpredictable way on the mixing ratio. For example, if we add (numerically) 10% of a Mn(II) edge spectrum (of $MnCO_3$) to each of the spectra shown in Figure 3, we obtain a downshift of the inflection point energies by 0.6, 1.2 (!), 0.2, and 0.0 eV for the S_0-,

Table 3: Edge Shifts for Deconvoluted Spectra (for Excitation at 55°)

method	E_1[a]	$E_1 - E_0$[b]	$E_2 - E_1$[b]	$E_3 - E_2$[b]	$E_0 - E_3$[b]
(1) integral[c]	6551.9	1.0	0.6	1.0	−2.6
(2) sec. derivative[d]	6553.0	2.4	0.8	0.7	−3.9
(3) half-of-norm height[e]	6551.3	1.1	0.7	1.1	−2.9
(4) half-of-peak height[f]	6552.8	1.3	0.8	0.8	−2.8

[a] Edge position for the S_1-state in eV. [b] Edge-shifts in eV. [c] Integral method described in Materials and Methods. [d] Zero crossing of the second derivative. [e] Energy corresponding to normalized absorption of 0.5. [f] Energy corresponding to normalized absorption of 0.65.

S_1-, S_2-, and S_3-states, respectively, resulting in edge shifts of 1.6, 1.9 (!), and 0.9 eV for the S_0-S_1, S_1-S_2, and S_2-S_3 transitions, respectively. Thus, with the use of the second-derivative method, minor contributions of adventitious Mn(II) to the spectra can cause an immense increase in the (apparent) S_1-S_2 edge shift (increase from 0.8 eV in the absence of Mn(II) to 1.9 eV for a 10% Mn contamination). Furthermore, the edge shifts obtained by the second-derivative method are highly dependent on the smoothing procedure used (*19*). In conclusion, the use of the second-derivative method for investigations of relatively small shifts in the X-ray edge position is problematic; its use by Roelofs et al. (*11*) presumably contributes to the discrepancies between the results presented here and in ref *11*.

Magnitude of Edge Shifts. We find a shift of the inflection point by 0.8 eV for the S_1-S_2 transition, whereas Roelofs et al. (*11*) determined the S_1-S_2 inflection point shift to be 1.8 eV. Creation of the S_2-state by continuous illumination at 200 K typically results in an S_1-S_2 edge shift of 0.8−1.0 eV (*25*−*28*). X-ray data obtained for synthetic manganese compounds is suggestive that (in the absence of significant changes in the manganese ligand environment) the detectable edge shift for the Mn(III)−Mn(IV) oxidation of one manganese ion of the PS II manganese complex is 0.5−1.0 eV (*9*, *29*−*31*). In conclusion, the S_1-S_2 edge shifts determined in the present investigation are of reasonable magnitude.

Mn Oxidation States. Investigations on UV absorption changes have mostly been interpreted as being indicative of Mn oxidation upon the S_2-S_3 transition as reviewed in ref *8*. Also, the occurrence of manganese oxidation provides a straightforward explanation for the absence of a readily detectable EPR multiline signal in the S_3-state. On the basis of EPR (*32*, *33*) and NMR relaxation studies (*34*), however, it has been proposed that the S_2-S_3 transition is not coupled to manganese oxidation. In ref *35* EPR results have been presented which appeared to prove the oxidation of a histidine residue for the S_3-state of Ca-depleted PS II. However, recent investigations seem to indicate that the EPR results described in ref *35* are not related to the formation of a histidine radical but rather to the accumulation of the Tyr_Z radical (*36*), a process which does not occur in PS II with an intact donor side. Reviewing various aspects of the controversy, Britt (*4*) and Penner-Hahn (*9*) conclude that the question of manganese oxidation in the S_2-S_3 transition is still unresolved.

Taking into consideration the uncertainty range of Table 1 and the variability stemming from the use of three different approaches for the determination of edge positions (methods (1), (3), and (4) in Table 3), we obtain an upshift of the edge position by 0.8−1.5, 0.5−0.9, and 0.6−1.3 eV for the S_0-S_1, S_1-S_2, and S_2-S_3 transitions, respectively, and a downshift by 2.3−3.1 eV for the S_3-S_0 transition. (The lower limit in each of the above ranges is the minimum of the values obtained by the methods (1), (3), and (4) minus the "likely error" of Table 1; the upper limit is the maximum of the three values plus the "likely error" of Table 1.) As discussed above, shifts in the position of the Mn K edge by 0.5 eV or more are suggestive of manganese oxidation state changes. Therefore we conclude that, most probably, the S_0-S_1, S_1-S_2, and the S_2-S_3 transitions are coupled to manganese-centered oxidation of the PS II manganese complex.

In Table 1, the edge shifts of the S_0-S_1 transition and the S_2-S_3 transition are significantly larger than the edge shift of the S_1-S_2 transition. Furthermore, the former transitions are coupled to particularly pronounced changes in the edge shape (Figure 3) and in the height of the pre-edge peak (feature around 6543 eV in Figure 3A). We tentatively propose that these observations are explainable by changes in the structure of the PS II manganese complex accompanying the oxidation state changes of the S_0-S_1 transition and the S_2-S_3 transition.

The results of various X-ray absorption investigations are suggestive of a $Mn(III)_2-Mn(IV)_2$ complex in the S_1-state and a $Mn(III)-Mn(IV)_3$ complex in the S_2-state (*2*, *3*, *10*). Consequently, we propose that the OEC in its S_3-state contains a $Mn(IV)_4$ complex.

With respect to the Mn oxidation state assignment in the S_0-state, the shoulder-like feature at 6555 eV in the S_0-spectrum marked by an arrow in Figure 3A is remarkable. We found that a comparable feature is always observed for PS II membrane particles previously exposed to treatments which induce the formation of Mn(II). Furthermore, various Mn(II) compounds exhibit a characteristic peak around 6554 eV (*3*). On the basis of this observation and taking into consideration that results of EPR studies also point toward the presence of Mn(II) in the S_0-state (*15*, *16*), we tentatively assume that the OEC in its S_0-state contains a $Mn(II)-Mn(III)-Mn(IV)_2$ complex.

In summary, we propose that photosynthetic oxygen evolution involves cycling of the PS II manganese complex through four distinct oxidation states of the tetranuclear manganese complex: $Mn(II)-Mn(III)-Mn(IV)_2$ in the S_0-state, $Mn(III)_2-Mn(IV)_2$ in the S_1-state, $Mn(III)_1-Mn(IV)_3$ in the S_2-state, and $Mn(IV)_4$ in the S_3-state. With the assumption of the validity of this oxidation state assignment, it is conceivable that in the S_4-state, before oxygen release takes place, an intermediate is formed which is a $Mn(IV)_3-Mn(V)$ complex.

ACKNOWLEDGMENT

We are grateful to Drs. H. Senger, D. Dörnemann, R. Schulz, and A. Batschauer (Marburg) for supporting this investigation in various ways. We thank Drs. O. Burghaus

and C. Elschenbroich (Marburg) for support with respect to the EPR measurements. We thank the staff of the mechanics workshop of the FB Biologie for the skillful making of XALDS sample holders and centrifuge tubes. We acknowledge the support of Drs. H. Schiller (Frankfurt), V. A. Solé (Grenoble), and H.-F. Nolting (Hamburg) in initial X-ray measurements related to this investigation. H.D. thanks Drs. K. Sauer, M. Klein, and V. Yachandra (Berkeley) and Dr. T. Roelofs (Berlin) for the joint investigations in 1992, which stimulated this work.

REFERENCES

1. Debus, R. J. (1992) *Biochim. Biophys. Acta 1102*, 269−352.
2. Yachandra, V. K., DeRose, V. J., Latimer, M. J., Mukerji, I., Sauer, K., and Klein, M. P. (1993) *Science 260*, 675−679.
3. Riggs-Gelasco, P. J., Mei, R., and Penner-Hahn, J. E. (1995) *Adv. Chem. Ser. 246*, 219−248.
4. Britt, R. D. (1996) in *Oxygenic Photosynthesis: The Light Reactions* (Ort, D. R., and Yocum, C. F., Eds.) pp 137−164, Kluwer Academic Publishers, Dordrecht, The Netherlands.
5. Yachandra, V. K., Sauer K., and Klein M. P. (1996) *Chem. Rev. 96*, 2927−2950.
6. Hoganson, C. W., and Babcock, G. T. (1997) *Science 277*, 1953−1956.
7. Kok, B., Forbush, B., and McGloin, M. (1970) *Photochem. Photobiol. 11*, 457−475.
8. Dekker, J. P. (1992) in *Manganese Redox Enzymes* (Pecoraro, V. L., Ed.) pp 85−103, VCH Publishers, New York.
9. Penner Hahn, J. E. (1998) in *Metal Sites in Proteins and Models Redox Centres* (Hill, H. A. O., Sadler, P. J., and Thomson A. J., Eds.) pp 1−36, Springer-Verlag, Heidelberg, Germany.
10. Ono, T., Noguchi, T., Inoue, Y., Kosunoki, M., Matsushita, T., and Oyanagi, H. (1992) *Science 258*, 1335−1337.
11. Roelofs, T. A., Liang, W., Latimer, M. J., Cinco, R. M., Rompel, A., Andrews, J. C., Sauer, K., Yachandra, V. K., and Klein, M. P. (1996), *Proc. Natl. Acad. Sci. U.S.A. 93*, 3335−3340.
12. Dismukes, G. C., and Siderer, Y. (1981) *Proc. Natl. Acad. Sci. U.S.A. 78*, 274−278.
13. Schiller, H., Dittmer, J., Iuzzolino, L., Dörner, W., Meyer-Klaucke, W., Sole, V. A., Nolting, H.-F., and Dau, H. (1998) *Biochemistry 37*, 7340−7350.
14. Schiller, H., Iuzzolino, L., Dittmer, J., and Dau, H. (1996) *Ber. Bunsen-Ges. Phys. Chem. 100*, 1999−2002
15. Messinger, J., Robblee, J. H., Yu, W. O., Sauer, K., Yachandra, V. K., and Klein, M. P. (1997) *J. Am. Chem. Soc. 119*, 11349−11350.
16. Åhrling, K. A., Peterson, S., and Styring, S. (1997) *Biochemistry 36*, 13148−13152.
17. Iuzzolino, L., Dittmer, J., Dörner W., and Dau, H. (1998) in *Proceedings of the XIth International Congress on Photosynthesis* (Garab, G., Ed.) Kluwer Academic Publishers, Dordrecht, The Netherlands (in press).
18. Schneider, F., and Plato, M. (1971) *Elektronen-Spin-Resonanz, Thiemig Taschenbücher Band 40*, Verlag Karl Thiemig, München.
19. Dittmer, J., Iuzzolino, L., Dörner, W., Nolting, H.-F., Meyer-Klaucke, W., and Dau, H. (1998) in *Proceedings of the XIth International Congress on Photosynthesis* (Garab, G., Ed.) Kluwer Academic Publishers, Dordrecht, The Netherlands (in press).
20. Shinkarev, V. P., and Wraight, C. A. (1993) *Photosynth. Res. 38*, 315−321.
21. Dau, H., Dittmer, J., Iuzzolino, L., Schiller, H., Dörner, W., Heinze, I., Sole, V. A., and Nolting, H.-F. (1997) *J. Phys. IV France 7, C2*, 607−610.
22. Mukerji, I., Andrews, J. C., DeRose, V. J., Latimer, M. J., Yachandra, V. K., Sauer, K., and Klein, M. P. (1994) *Biochemistry 33*, 9712−9721.
23. Pettifer, R. F., Brouder, C., Benfatto, M., Natoli, C. R., Hermes, C., and López, M. F. R. (1990) *Phys. Rev. B: Condens. Matter 42*, 37−42.
24. Dittmer, J., and Dau, H. (1998) *J. Phys. Chem*. (in press).
25. Liang, W., Latimer, M. J., Dau, H., Roelofs, T. A., Yachandra, V. K., Sauer, K., and Klein, M. P. (1994) *Biochemistry 33*, 4923−4932.
26. Guiles, R. D., Zimmermann, J. L., McDermott, A. E., Yachandra, V. K., Cole, J. L., Dexheimer, S. L., Britt, R. D., Wieghardt, K., Bossek, U., Sauer, K., and Klein, M. P. (1990) *Biochemistry 29*, 471−485.
27. Guiles, R. D., Yachandra, V. K., McDermott, A. E., Cole, J. L., Dexheimer, S. L., Britt, R. D., Sauer, K., and Klein, M. P. (1990) *Biochemistry 29*, 486−496.
28. MacLachlan, D. J., Nugent, J. H. A., and Evans, M. C. W. (1994) *Biochim. Biophys. Acta 1185*, 103−111.
29. Kirby, J. A., Goodin, D. B., Wydrzynski, T., Robertson, A. S., and Klein, M. P. (1981) *J. Am. Chem. Soc. 103*, 5537−5542.
30. Sauer, K., Yachandra, V. K., Britt, R. D., and Klein, M. (1992) in *Manganese Redox Enzymes* (Pecoraro, V. L., Ed.) pp 85−103, VCH Publishers, New York.
31. Bossek, U., Hummel, H., Weyhermüller, T., Wieghardt, K., Russel, S., van der Wolf, L., and Kolb, W. (1996) *Angew. Chem. 108*, 1653−1656.
32. Styring, S. A., and Rutherford, A. W. (1988) *Biochemistry 27*, 4915−4923.
33. Evelo, R. G., Styring, S. A., Rutherford, A. W., and Hoff, A. J. (1989) *Biochim. Biophys. Acta 973*, 428−442.
34. Sharp, R. R. (1992) in *Manganese Redox Enzymes* (Pecoraro, V. L., Ed.) pp 85−103, VCH Publishers, New York.
35. Boussac, A., Zimmermann, J.-L., Rutherford, A. W., and Lavergne, J. (1990) *Nature 347*, 303−306.
36. Tang, X.-S., Randall, D. W., Force., D. A., Diner, B. A., and Britt, R. D. (1996) *J. Am. Chem. Soc. 118*, 7638−7639.

BI9817360